*Journal of Energy Research and Reviews*

*12(4): 1-14, 2022; Article no.JENRR.92704*
*ISSN: 2581-8368*

# Effects of Mono-Halogen-Substitution on the Electronic and Non-Linear Optical Properties of Poly(3-hexylthiophene-2,5-diyl) for Solar Cell Applications: A DFT Approach

**Abubakar Maigari [a*], A. B. Suleiman [b], A. S. Gidado [c] and Chifu E. Ndikilar [b]**

*[a] Department of Physics, Aminu Saleh College of Education Azare, Bauchi State, Nigeria.*
*[b] Department of Physics, Federal University Dutse, Jigawa State, Nigeria.*
*[c] Department of Physics, Bayero University Kano, Kano State, Nigeria.*

***Authors' contributions***

*This work was carried out in collaboration among all authors. All authors read and approved the final manuscript.*

***Article Information***

DOI: 10.9734/JENRR/2022/v12i4243

**Open Peer Review History:**
This journal follows the Advanced Open Peer Review policy. Identity of the Reviewers, Editor(s) and additional Reviewers, peer review comments, different versions of the manuscript, comments of the editors, etc are available here: https://www.sdiarticle5.com/review-history/92704

***Original Research Article***

***Received 09 August 2022***
***Accepted 19 October 2022***
***Published 25 October 2022***

## ABSTRACT

Poly(3-hexylthiophene-2,5-diyl) with the acronym P3HT and its derivatives are p-type conjugated semiconductor polymers that have been proved to be good organic semiconductors. They have several applications in many areas, such as photovoltaic systems, organic light-emitting diodes, and so on. The instability of organic molecules under ambient conditions is one factor deterring the commercialization of such organic semiconductor devices. Here we present a theoretical study using density functional theory (DFT) approach with Gaussian 09 and GaussView 5.0, to investigate the effects of halogens (Bromine, Chlorine, Fluorine and Iodine) on the electronic and nonlinear optical properties of poly(3-hexylthiophene-2,5-diyl) (P3HT). This is to enable us to address the issue of instability in the molecule. The bond lengths and bond angles of the mono-halogenated molecules were found to be less than that of the isolated Poly(3-hexylthiophene-2,5-diyl). Iodine doped P3HT was found to be the most stable amongst the studied molecule for having the least bond angles and bond lengths. The calculated band gap for iodine doped P3HT and fluorine doped P3HT were observed to have the lowest energy gap of 3.519 eV and 3.545 eV respectively thus proving that iodine doped P3H is the most stable and this makes it more suitable

**Corresponding author: E-mail: maigaria2022@gmail.com, malallami2014@gmail.com;*

for photovoltaic applications. The molecule with the highest value of chemical hardness was obtained to be the isolated P3HT with a chemical hardness of 1.937eV. This is followed by bromine doped P3HT, chlorine doped P3HT, fluorine doped P3HT and iodine doped P3HT with values as 1.925 eV, 1.813 eV, 1.773 eV, and 1.7595 eV respectively. All the substituted molecules results were found to be more reactive than their isolated form for having lower values of chemical hardness. The results for the nonlinear optical (NLO) properties show that the first-order hyper-polarizability of chlorine doped P3HT and iodine doped P3HT as $2.9876 \times 10^{-30}\ esu$ and $2.8803 \times 10^{-30} esu$ respectively were found to be about eight times more than that of the urea value (0.3728 x$10^{-30}$ esu), which is commonly used for the comparison of NLO properties with other materials. This makes them very good NLO materials. The open circuit voltage ($V_{oc}$) was also calculated. The highest values of the calculated open circuit voltage ($V_{oc}$) were found to be $1.3629$ eV (PCBM $C_{60}$) in chloroP3HT and 1.3134 eV (PCBM $C_{60}$) in flouroP3HT. The results of the IR frequency show that the doped molecules are more stable than the isolated molecule. Zero-point vibrational energy (ZPVE), total entropy (S) and molar heat capacity (Cv) were also calculated and presented. We also observe that the entropy and heat capacity of the doped materials are higher than those of the original molecule, which confirms that the charge dynamics of the doped molecules are higher than those of the original molecule at the same temperature. This result further demonstrates that these doped materials have a high chemical reactivity and a high thermal resistivity, hence their application in the fields of organic electronics. By and large the overall results confirm that there is a good electron transfer within the doped molecules which makes them have potential applications in photovoltaic devices.

*Keywords: Poly(3-hexylthiophene-2,5-diyl); DFT; halogens; NLO and PCBM $C_{60}$.*

## 1. INTRODUCTION

"Conjugated polymers are of appreciable interest due to their electronic properties and their potential technological applications" [1]. "They have many advantages compared to inorganic semiconductors, such as easy processing and tunable optical gaps. Their electronic properties are determined by the delocalized $\pi$-electrons along their carbon backbone" [2]. "Polythiophene is the most useful conjugated polymer utilized in a broad spectrum of applications such as conducting polymers, light-emitting diodes, field effect transistors, and plastic solar cells, due to its outstanding optical and electrical properties as well as exceptional thermal and chemical stability. Originally, the applications of non-substituted Polythiophene were very insubstantial because of its insolubility in many organic solvents, due to its extended conjugated structure. Moreover, the alkyl chain has been incorporated into the thiophene units to obtain a functional monomer able to yield soluble polymers. The poly(3-hexylthiophenes) evolved to be highly producible conducting polymers whose solubility allowed their full characterization by spectroscopic method" [3]. "Poly (3-hexylthiophene-2,5 diyl) belongs to the poly(3alkylthiophene) family with a molecular formula ($C_{10}$ $H_{14}$)n. P3HT has been studied as a promising material for applications in solar cells, light-emitting diodes, displays, or other optoelectronic devices due to its processability, flexibility, and low production costs"[4]. "Moreover, many important aspects of the electronic and optical properties of these materials are still not fully resolved" [5]. "Poly-3-hexylthiophene (P3HT) was widely used as the hole transport layers (HTL) due to its low cost and doping-free features" [6]. "However, in the beginning, the efficiency of P3HT HTL based PSC can be attributed to the fact that the flat P3HT molecule is easy to cause substantial charge recombination due to the close contact between the thiophene units and perovskite" [7]. "Besides, the device based on the P3HT HTL has a low open circuit voltage ($V_{OC}$) which can be ascribed to the high occupied molecular orbital (HOMO) energy level" [8]. "Due to the hole mobility of P copolymer (1.95 $cm^2 \cdot V^{-1} \cdot S^{-1}$) which is greater than that of P3HT ($3 \times 10^{-4}$ $cm^2 \cdot V^{-1} \cdot S^{-1}$), the device-based P HTL had an efficiency of $10.8\%$, more than that of P3HT HTL $(6.62\%)$. However, the device efficiency based on the P3HT is always less than that based on Li-doped Spiro-OMeTAD, which can be ascribed to the low hole mobility of P3HT" [9]. "Several efforts have been made to adjust and improve the hole mobility of P3HT, such as adding the additives or fabricating the composites of P3HT/carbon materials" [9,10].

"Optical and electronic properties of organic semiconductor materials may be easily adjusted

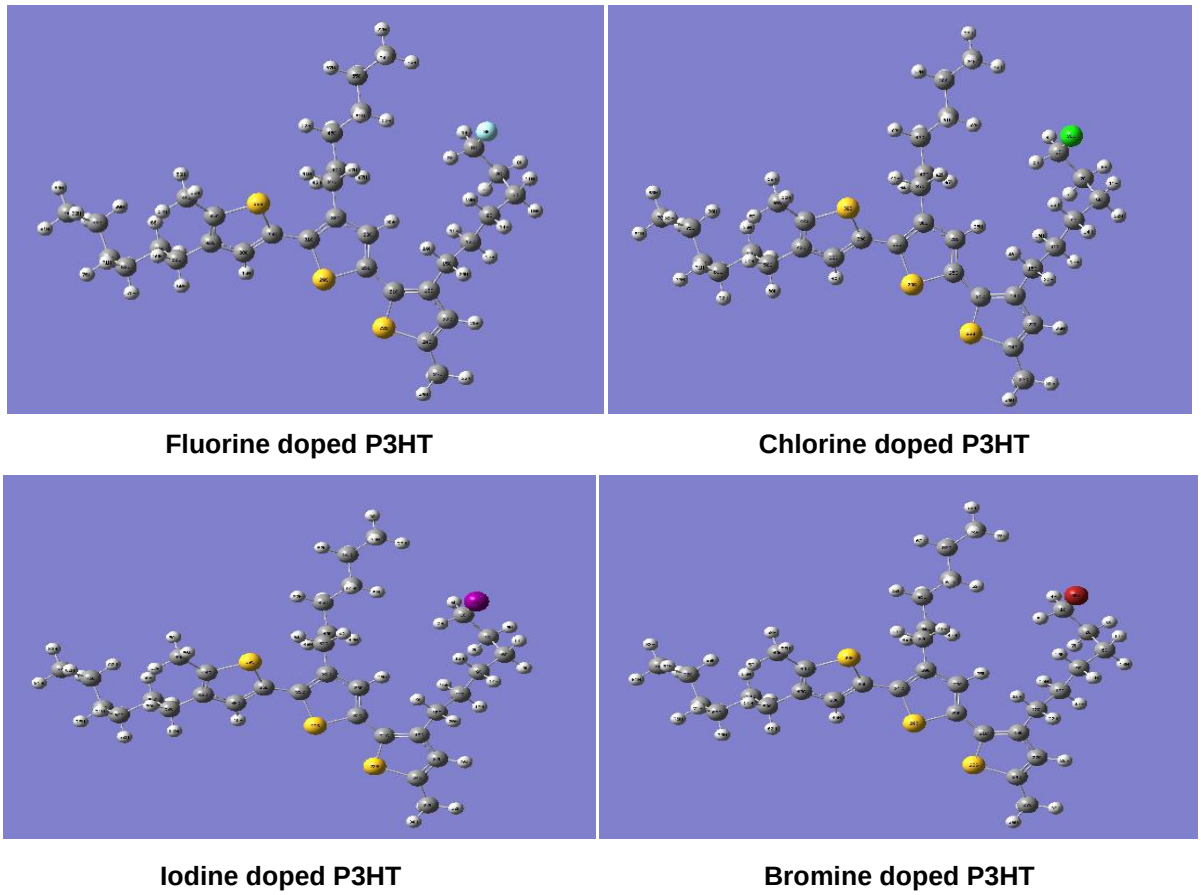


**Fig. 1. Optimized structures of doped poly(3-hexylthiophene-2,5-diy**

and tuned through chemical modifications. For instance, fluorine (F) substituent was attached to conjugated polymer donor materials for the purpose of lowering the LUMO energies and of increasing the open-circuit voltage in various polymers such as, PTB7, although the efficiency decreased due to poor compatibility of the derivative with PC61BM; PCDTBT, where a 25% increase in efficiency was observed using end-group fluorination; and BDT– DTBT, where as high as 75% increase in efficiency was observed for the fluorinated derivative" [11]. "However, lowering the LUMO energies using F were observed to be very limited in conjugated polymers with high intrinsic HOMO energies. Therefore, studies on stronger electron-withdrawing substituents are very much desired to improve thiophene-based and related materials for organic solar cells" [11]. "Quantum chemical studies based on density functional theory (DFT) have been fortunate in evaluating the optical and electronic properties of π-conjugated systems. Even though the results of DFT calculations were observed to deviate from the experimental values for these systems, the trends in the results were found to agree with the experimental findings. Thus, changes in the properties resulting from the chemical modifications can be satisfactorily addressed using this method" [11]. In the work of [12], an investigation of HOMO, LUMO and band-gap of poly (3-hexyltylthiophene-2,5 diyl) using synthesized of a series of highly regioregular fluorinated P3HT-based homopolymers via iterative thiophene couplings was carried out and it was reported that, the HOMO, LUMO, and band-gap energy of P3HT are -5.69eV, -1.34eV and 4.35eV respectively. Furthermore, spectrophotometry and ellipsometry methods were used to investigate the basic optical parameters and electronic structure of conjugated polymer. Their report discovered that P3HT and P3OT had band-gap energies of 2.43eV and 2.51eV respectively [12]. Also, DFT and TD-DFT studies have been applied for several organic molecules such as Cyanidin [13], Phenylenevinylene [14], Aceantraquinoxaline [15], Triphenylamine [16]), Thionopyrazine and thiophene [17], thiophene, and benzene [18] for solar cell applications. DFT- based calculations

have been significant in understanding the electronic properties of different systems on an atomic scale thus aiding experimentalists in the design, prediction, and functionalization of different materials necessary for a specific application. To the best of our knowledge, there was no report on doping with iodine and bromine for this particular molecule, despite their importance in tuning the properties of polymer organic semiconductors.

To address the above gap, we investigated the effects of doping Poly(3-hexylthiophene-2,5-diyl) with halogens (F, Cl, Br, and I) with the aim of shedding more light on its optoelectronics and non-linear optical properties for photovoltaic applications. Due to their high electronegativity and electron affinity, halogens are electron withdrawing groups.

## 2. THEORETICAL BACKGROUND

### 2.1 Density Functional Theory

"Density functional theory refers to variational method that is currently one of the most successful mechanism for calculating the electronic structure of matter. Its relevancy ranges from atoms, molecules, and solids to nuclei, quantum, and classical fluids. The density functional theory is derived from the N-particle Schrodinger equation and is expressed in terms of the density distribution of the ground state and the single-particle wave function"[19]. "The applicability of DFT ranges from atoms, molecules and solids to nuclei and quantum and classical fluids. DFT predicts a great variety of molecular properties: molecular structures, vibrational frequencies, atomization energies, ionization energies, electric and magnetic properties, reaction paths and so on" [20-21].

"Density functional approach is based on a strategy of modelling the electron correlation via general functional of the electron density. Following the work by Kohn and Sham, the approximate functional employed by current DFT methods separate the electronic energy into several terms" [20-21].

$$E = E_T + E_V + E_J + E_{XC} \quad (1)$$

where $E_T$ is the kinetic energy term, $E_V$ includes terms describing the potential energy of the nuclear-electron attraction and of the repulsion between pairs of nuclei, $E_J$ is the electron-electron repulsion term, and $E_{XC}$ is the exchange-correlation term and includes the remaining part of the electron-electron interactions.

Hohenberg and Kohn demonstrated that $E_{XC}$ is entirely determined by the electron density:

$E_{XC}(\rho) = \int f\,(\rho_\alpha(r), \rho_\beta(r), \nabla\rho_\alpha(r), \nabla\rho_\beta(r))d^3(r)$ (2)
where $\rho_\alpha$, $\rho_\beta$ are referring to the corresponding α, β spin densities.

$E_{XC}$ is usually divided into components, referred to as the *exchange* and *correlation* parts, but actually corresponding to the same-spin and mixed-spin interactions, respectively:

$$E_{XC}(\rho) = E_X(\rho) + E_C(\rho) \quad (3)$$

### 2.2 Vibrational Frequency

The vibrational frequencies are calculated with the following equations [21]:

$$V_{ij} = \frac{1}{\sqrt{m_i m_j}}\left(\frac{\partial^2 V}{\partial_{qi}\partial_{qj}}\right) \quad (4)$$

Where $V_{ij}$ is the Hessian matrix, $m_i$ refers to the mass of atom i, *and* $\partial_{qi}$ refers to a displacement of atom *i* in the x-, y-, or z-direction,

$$\text{Thus } VU = \lambda U \quad (5)$$

Where *U is* a matrix of eigenvectors and $\lambda$ is a vector of eigenvalues, and

$$\lambda_k = (2\pi v_k)^2 \quad (6)$$

where $\lambda_k$ is the $k^{th}$ eigenvalue and $v_k$ is the $k^{th}$ vibrational frequency.

The infrared intensities can be computed with the equation [21]

$$\frac{\partial E_{SCF}}{\partial f \partial a} = 2\sum_i^{d.o} h_{ij}^{fa} + 4\sum_i^{d.o}\sum_j^{all} U_{ji}^a h_{ij}^f \quad (7)$$

where

$$h_{ij}^{fa} = \sum_{\mu\upsilon}^{AO} C_\mu^{i0} C_\upsilon^{i0}\left(\frac{\partial^2 h_{\mu\upsilon}}{\partial f \partial a}\right) \quad (8)$$

$E_{SCF}$ is the self-consistent field energy, *f* is the electric field, *a* is a nuclear coordinate, $h_{\mu\upsilon}$ is the one-electron atomic orbital integral, $U^a$ is related to the derivative of the molecular orbital coefficients with respect to *a* by

$$\frac{\partial C_\mu^i}{\partial a} = \sum_m^{all} U_{mi}^a C_\mu^{m0} \quad (9)$$

## 2.3 Global Reactivity Descriptors

The global reactivity descriptors such as chemical potential, chemical hardness-softness, electronegativity and electrophilicity index are useful parameters in predicting and understanding global chemical reactivity trends. The ionization potentials (IP) and electron affinities (EA) of the molecule are computed using Koopman's Hypothesis, through the HOMO and LUMO energy orbitals respectively using the following expressions [22,23]:

$$IP = -E_{HOMO} \quad \text{and} \quad EA = -E_{LUMO} \tag{10}$$

The difference between the highest occupied molecular orbital (HOMO) and lowest unoccupied molecular orbital (LUMO) is known as energy gap can be calculated from the relation;

$$E_{Gap} = E_{LUMO} - E_{HOMO} \approx IP - EA \tag{11}$$

The chemical hardness $(\eta)$ and chemical hardness $(S)$ are obtained from the equations

$$\eta = \frac{IP-EA}{2} \quad \text{and} \quad S = \frac{1}{\eta} \tag{12}$$

The chemical potential $(\mu)$ and electronegativity $(\chi)$ are also given by

$$\mu = -\left(\frac{IP + EA}{2}\right) \quad \text{and} \quad \chi = \frac{IP+EA}{2} \tag{13}$$

The electrophilic index is expressed as

$$\omega = \frac{\mu^2}{2\eta} \tag{14}$$

## 2.4 Open-Circuit Voltage $(V_{oc})$

The open-circuit voltage$(V_{oc})$ is one of the most important parameters that determines the efficiency of Organic solar cells (OSCs) and represents the maximum voltage a solar cell can provide to an external circuit. The maximum open-circuit voltage (Voc) is obtained from the difference between the HOMO of the donor (π-conjugated molecule) and the LUMO of the acceptor, taking into cognizance the energy lost during the photo-charge generation. The theoretical values of the open-circuit voltage of organic bulk heterojunction (BHJ) solar cell are calculated from [14].

$$V_{OC} = E_{HOMO}^{Donor} - E_{LUMO}^{Acceptor} - 0.3 \tag{15}$$

where the value of 0.3 V is an empirical factor.

## 2.5 Non-Linear Optical (NLO) Properties

To have a clearer picture for the study of the non-linear optical properties (NLO) of poly(3-hexylthiophene-2,5-diyl) (P3HT) and its substituted molecules; the dipole moment (μ), polarizability $(\alpha)$, anisotropic polarizability $(\Delta\alpha)$, and hyperpolarizabilities $(\beta \; and \; \gamma)$ were computed at DFT/B3LYP with 6-311++G (d, p) basis set.

For molecular systems, the dipole moment can be obtained from [24];

$$\mu_{\text{tot}} = \left[\mu_x + \mu_y + \mu_z\right]^2 \tag{16}$$

Where $\mu_x$ , $\mu_y$ and $\mu_z$ are the components of dipole moment in x, y and z coordinates

Electric dipole polarizability is given by [25];

$$\alpha = \frac{\partial^2 E}{\partial F_a \partial F_b} \tag{17}$$

where a and b are coordinates of x, y, and z.

The mean polarizability is calculated using [26];

$$< \alpha > = \frac{1}{2}\left(a_{xx} + a_{yy} + a_{zz}\right) \tag{18}$$

where $a_x$, $a_y$, and $a_z$ are quantities known as principal values of polarizability tensor.

The anisotropic polarizability is given by [27];

$$\Delta\alpha = \frac{1}{\sqrt{2}}\left[\left(a_{xx} - a_{yy}\right)^2 + \left(a_{yy} - a_{zz}\right)^2 + (a_{zz} - a_{xx})^2 + 6\left(a_{xz} + a_{xy} + a_{yz}\right)\right]^{1/2} \tag{19}$$

Similarly the first order hyperpolarizability is defined as [23];

$$\beta = \left[\left(\beta_{xxx} + \beta_{yyy} + \beta_{zzz}\right)^2 + \left(\beta_{yyy} + \beta_{yzz} + \beta_{yxx}\right)^2 + \left(\beta_{zzz} + \beta_{xzz} + \beta_{zyy}\right)^2\right]^{1/2} \tag{20}$$

The second order hyperpolarizability is given by [28];

$$\gamma = \frac{1}{5}\left[\gamma_{xxxx} + \gamma_{yyyy} + \gamma_{zzzz} + 2\left(\gamma_{xxyy} + \gamma_{xxzz} + \gamma_{yyzz}\right)\right] \tag{21}$$

## 3. COMPUTATIONAL METHODOLOGY

The molecular geometries of poly(3-hexylthiophene-2,5-diyl) and halogens ( chlorine, bromine, fluorine, and iodine) doped poly(3-hexylthiophene-2,5-diyl) were completely optimized without any constraint based on the analytical gradient procedure of density functional theory (DFT) as implemented in Gaussian 09 program with b3lyp/6-311++G(d,p) level of theory [29]. The DFT method was proved to be one of the most accurate methods for the computation of the electronic structure of molecules and solids [30-32]. Geometry optimization was performed until the lowest energy geometry was obtained. The optimized geometries were then used to compute the bond parameters, HOMO energy, LUMO energy, entropy (S) and the specific heat capacity ($C_V$). The frontier MOs (HOMO and LUMO) were used to calculate the energy gap $(E_g)$ , ionization potential (IP) , electron affinity (EA) and global chemical index parameters using equations 10-13 . At the same level of theory, dipole moment (μ), isotropic polarizability ($\alpha$), anisotropic polarizability (Δα) and first order polarizability ($\beta$) and second order polarizability of the investigated molecules were also computed using the same optimized geometries using equations 16-21. The optimized geometry obtained was used as the starting point for frequency calculations. The IR frequencies were calculated by obtaining the Hessian matrix and the force constants for all the normal modes of the molecule. The spectra of the molecules were plotted using GaussSum 3.0 Software. Gaussian predicted the frequencies and intensities of each spectral line. Analysis of the spectra was done using IRPal 2.0 software [ 33].

## 4. RESULTS AND DISCUSSION

### 4.1 Optimized Bond Angles

In Tables 1 and 2, some of the selected values of the bond lengths and bond angles based on their strengths and weaknesses, of the parent and doped molecules computed at DFT/B3LYP level using 6311++G (d, p) basis set are presented. The bond length measures the distance between two atoms covalently bonded together. In accordance with the molecular orbital (MO) theory, covalent bonds are considered to be formed from the overlap of two atomic orbitals. "During overlapping, if the force of attraction between the atoms is balanced by the force of repulsion between the nuclei of two atoms, then the equilibrium distance between the two atomic nuclei is called bond length" [34]. It is important to note that, if the bond length is smaller, then the bond energy is stronger. In a molecule, two atoms remain closer to each other so that the system has a minimum energy [35]. From Table 1, the substitution of halogen atoms to the isolated P3HT molecule shows that there are little changes in the bond lengths. The result shows that the smallest value obtained was 1.0812Å in iodine doped P3HT ($C_{30}$-$C_{37}$) using 6-311++G (d, p) basis set. However, comparing the results obtained with that of an isolated P3HT molecule, the bond length in iodine doped P3HT molecule tends to be a little bit smaller which implies it has the strongest bond energy than the other substituted molecules. It is found that the bonds $C_{40}$-$H_{47}$ for all the molecules at the indicated positions have the lowest values of the bond lengths ranging between 1.0829Å and 1.0859Å. These are the strongest bonds and have the largest bond energy in the substituted P3HT molecules which cannot be disintegrated easily. A large amount of energy is required to break them. This shows that the presence of halogen atoms shorten the bond lengths in most cases and thus increases the bond energy of the titled molecule. The bond lengths are found to be in good agreement with those from previous work [36].

#### 4.1.1 Selected bond angles (˚) of the optimized structure of Isolated and substituted P3HT

The optimized bond angles of P3HT molecule of isolated P3HT and substituted P3HT are listed in Table 2. The bond angle is the mean angle between the orbitals of the central atom containing the bonding electron pairs in the molecule and is measured in degrees [37]. "It is also the internal angle between the orbital-containing electron pairs in the valence shell of the central atom in a covalent molecule" [38]. The bond angle gives more information about the distribution of orbitals around a central atom in a molecule. The bond angles also throw more light on the shape of a molecule. From the results, the value obtained for iodine doped P3HT is $129.9863^0$ ($C_{18}$-$C_{22}$-$H_{26}$) which is a bit bigger than the ones obtained in the other substituted molecules with $122.6588^0$, $129.3996^0$, $122.3481^0$, and then $122.0079^0$ for fluorine, bromine, chlorine doped P3HT and isolated P3HT respectively. The bond angles are found to be closer to $120^0$, showing that the molecule is sp2 hybridized benzene. The bond bond angles are found to be in good agreement with those of previous work [36].

**Table 1. Selected bond Lengths in (Å) of the optimized structure of isolated and substituted P3HT molecules using B3LYP with 6-311++G (d, p) basis set**

| Bond length | Isolated P3HT | Bromine doped P3HT | Chlorine doped P3HT | Fluorine doped P3HT | Iodine P3HT | Previous works [35] |
|---|---|---|---|---|---|---|
| $C_1$-$C_2$ | 1.5443 | 1.522 | 1.5222 | 1.529 | 1.5309 | 1.55 |
| $C_1$-$H_3$ | 1.0966 | 1.9899 | 1.9219 | 1.4299 | 2.2314 | |
| $C_l$-$H_4$ | 1.0956 | 1.0899 | 1.0885 | 1.0954 | 1.0894 | 1.02 |
| $C_l$-$H_5$ | 1.0954 | 1.0899 | 1.088 | 1.0961 | 1.0897 | |
| $C_2$-$H_3$ | 1.5485 | 2.9343 | 1.7349 | 1.5249 | 3.1676 | |
| $C_2$-$C_6$ | 1.0967 | 1.7343 | 1.5453 | 1.547 | 1.1679 | |
| $C_2$-$H_7$ | 1.0978 | 1.5381 | 1.0995 | 1.0955 | 1.5462 | |
| $C_2$-$H_8$ | 1.5481 | 1.1005 | 1.0957 | 1.0962 | 1.1001 | |
| $H_3$-$H_4$ | 1.0987 | 2.5011 | 1.5349 | 1.0349 | 2.7125 | |
| $H_3$-$H_5$ | 1.0988 | 2.4967 | 1.5344 | 1.5349 | 2.7208 | 1.88 |
| $C_{30}$-$C_{37}$ | 1.8316 | 1.0838 | 1.5154 | 1.5148 | 1.0812 | |
| $C_{40}$-$H_{47}$ | 1.5146 | 1.0859 | 1.0982 | 1.0976 | 1.0829 | |
| $C_1$-$C_2$ | 1.5432 | 1.5211 | 1.5248 | 1.5194 | 1.3307 | 1.37 |
| $S_{23}$-$C_{24}$ | 1.8238 | 1.745 | 1.752 | 1.7521 | 1.4354 | 1.43 |
| $C_{75}$-$H_{79}$ | 1.0964 | 1.5345 | 1.0981 | 1.0981 | 1.5486 | |
| $C_{75}$-$H_{80}$ | 1.0921 | 1.0989 | 1.0967 | 1.0967 | 1.0982 | |

**Table 2. Selected bond angles in (˚) of the optimized structure of isolated and substituted P3HT molecules by using B3LYP with 6-311++G (d, p) basis sets**

| Bond angles | Isolated P3HT | Bromine doped P3HT | Chlorine doped P3HT | Fluorine doped P3HT | Iodine doped P3HT | Previous works [36] |
|---|---|---|---|---|---|---|
| $C_2$-$C_1$-$H_3$ | 110.4374 | 112.0545 | 110.1797 | 108.5559 | 111.9039 | |
| $C_2$-$C_1$-$H_4$ | 110.8928 | 112.903 | 112.9538 | 111.0952 | 112.5913 | 113.00 |
| $C_2$-$C_1$-$H_5$ | 111.3079 | 109.3531 | 114.0125 | 110.82 | 109.4881 | |
| $H_3$-$C_1$-$H_4$ | 108.2083 | 116.0622 | 103.8138 | 109.0266 | 115.1822 | 115.00 |
| $H_3$-$C_1$-$H_5$ | 108.1356 | 105.964 | 104.0816 | 108.7532 | 106.4316 | |
| $H_4$-$C_1$-$H_5$ | 107.7385 | 109.0134 | 110.9253 | 108.5439 | 109.3185 | |
| $C_1$-$C_2$-$C_6$ | 113.1263 | 91.8443 | 114.33 | 110.9312 | 92.8401 | |
| $C_{18}$-$C_{22}$-$H_{26}$ | 122.0079 | 129.3996 | 122.3145 | 122.6588 | 129.9863 | 129.00 |
| $C_{24}$-$C_{22}$-$H_{26}$ | 122.1524 | 119.9739 | 92.2955 | 122.3181 | 120.4382 | |
| $C_{21}$-$S_{23}$-$C_{24}$ | 89.8807 | 114.9743 | 110.095 | 92.3024 | 115.8162 | |
| $C_{22}$-$C_{24}$-$S_{23}$ | 110.4075 | 122.6542 | 128.4456 | 110.0886 | 121.9843 | |
| $H_{57}$-$C_{49}$-$H_{58}$ | 107.9821 | 111.8456 | 113.5123 | 107.5219 | 111.4243 | |
| $C_{43}$-$C_{50}$-$C_{54}$ | 111.8686 | 107.5155 | 110.2859 | 113.4714 | 108.0401 | |
| $C_{43}$-$C_{50}$-$H_{59}$ | 110.3434 | 107.3488 | 108.9186 | 110.288 | 107.8397 | |
| $C_{43}$-$C_{50}$-$H_{60}$ | 109.1338 | 107.5427 | 108.9511 | 108.9492 | 108.0102 | |
| $C_{54}$-$C_{50}$-$H_{59}$ | 109.0994 | 113.3238 | 108.9093 | 108.9524 | 111.4941 | |
| $C_{54}$-$C_{50}$-$H_{60}$ | 108.9874 | 110.278 | 105.9811 | 108.9003 | 110.3717 | |
| $H_{56}$-$C_{50}$-$H_{60}$ | 107.1625 | 109.0471 | 113.2613 | 106.001` | 109.3324 | |
| $C_{45}$-$C_{51}$-$C_{55}$ | 112.4485 | 108.9798 | 110.1109 | 113.2829 | 109.1418 | |
| $C_{45}$-$C_{51}$-$H_{61}$ | 110.0413 | 108.9217 | 109.1231 | 110.1207 | 109.1964 | |

## 4.2 Molecular Orbital Energies (MOEs)

Table 3 presents the HOMO, LUMO, and HOMO-LUMO energy gaps of the isolated and substituted P3HT molecules calculated at the DFT/B3LYP level with 6-311++G (d, p) basis set. Lower values of HOMO-LUMO energy gap indicate a high kinetic energy and chemical reactivity. Thus, compounds with smaller HOMO-LUMO energy gap values show a tendency to have higher stability [35]. "Molecular orbitals when viewed in a qualitative graphical representation can provide insight into the nature of reactivity and some of the structural and

physical properties of molecules" [39]. The results obtained in Table 3 show that the presence of the substituted halogen atoms causes a slight decrease in the HOMO-LUMO energy gap of the isolated P3HT molecule except the bromine doped P3HT which has the highest energy gap. Thus, iodine doped P3HT has the lowest values of the energy gap of about 3.519 eV; followed by fluorine doped P3HT with 3.545 eV, chlorine doped P3HT with 3.626 eV and then bromine doped P3HT with 3.85eV. This shows that the iodine doped P3HT molecule has the lowest HOMOL-UMO energy gap, which implies kinetic energy is higher in the iodine substituted molecule. Therefore, iodine doped P3HT has much higher chemical reactivity than the other substituted P3HT molecules. A previously reported work obtained a higher band gap energy of 4.35 eV which indicates low stability compared to our doped molecule [40]. The values of ionization potential (IP) and electron affinity (EA) for isolated and halogen doped P3HT are also shown in Table 3.

### 4.3 Global Chemical Reactivity Parameters (GCRP)

GCR parameters of molecules such as hardness (η), softness (ʃ), chemical potential (μ), electronegativity (χ) and electrophilicity index (ω) of the isolated and doped P3HT are reported in Table 4. Chemical hardness is said to increase with the increase in the HOMO-LUMO energy gap. A molecule with higher chemical hardness is said to be more stable and less reactive. As seen in Table 4, bromine doped P3HT with a slightly higher value of chemical hardness of 1.925 eV is considered to be harder and more stable than the rest of the substituted molecules, followed by the isolated P3HT and chlorine doped P3HT with chemical hardness of $1.9137eV$ and $1.813eV$ respectively while fluorine doped P3HT and iodine doped P3HT have $1.773eV$ and $1.7595eV$ respectively. This shows that the substitution of bromine in the P3HT molecule makes it more stable than the rest of the halogen atoms. This indicates that the presence of the substituted halogen atoms increases the stability and chemical reactivity of the studied molecule.

### 4.4 Thermodynamic Properties

The thermodynamic parameters presented in Table 5 are zero-point vibrational energy (ZPVE), total entropy (S) and molar heat capacity (Cv), which arise from contributions of electronic, translational, rotational constants and vibrations. They were calculated at constant temperature and pressure of about $298.1K$ and $1atm$ respectively. The analysis of thermodynamic parameters is important in the estimation of the outcome of a chemical reaction [41]. Our findings show that halogen substitutions to the structure of P3HT improved the molar heat capacity (Cv) and entropy of the molecule compared to the isolated one which confirms that the charge dynamics of the doped molecules are higher than its original molecule at the same temperature [42]. This result further demonstrates that these doped materials have a high chemical reactivity and a high thermal resistivity, hence their application in the field of organic electronics.

Zero-point vibrational energy (ZPVE) was found to increase compared to the isolated molecule only when doped with fluorine. The results affirm that the doped molecules have higher chemical reactivity and thermal stability than the isolated P3HT molecule due to the increase in their kinetic energy.

### 4.5 Non-Linear Optical Properties

Nonlinear optics plays a key role in the current demand in global research, as NLO active materials find applications in data processing and storage, telecommunications, and potential applications in modern technologies, [43]. To understand the relationships between molecular structure and nonlinear optical properties, the mean and anisotropic polarizabilities, first and second-order hyperpolarizabilities of isolated P3HT and doped P3HT were calculated at DFT / B3LYP level using 6311++G(d,p) basis set. It is a well-known fact that higher values of dipole moment, polarizability, and hyperpolarizability are important for more active NLO materials. The calculated values for nonlinear optical properties parameters are presented in Table 6. It is observed from the table that there is an increase in values of total dipole moments ($\boldsymbol{\mu_{tot}}$), the total polarizability ($\boldsymbol{\alpha}_{\text{tot}}$), anisotropy of polarizability $\langle \boldsymbol{\Delta\alpha} \rangle$, first-order hyperpolarizability ($\boldsymbol{\beta_{tot}}$), and second order hyperpolarizability ($\boldsymbol{\gamma_{tot}}$), due to the effects of the substitutions. The significant increase in the dipole moments of the new materials leads to our belief that the substituted molecules are polar materials. Our finding reveals that the isolated P3HT molecule is neutral and does not exhibit nonlinear optical behavior. However, when substituted with halogen atoms (bromine, chlorine, and iodine) we realized that its first-order hyperpolarizability

($\beta_{tot}$), values turn out to be larger than (about eight times) that of the prototype urea (0.3728 x$10^{-30}$ esu) molecule, which is commonly used for the comparison of NLO properties with other materials. In view of the foregoing, this makes the doped materials excellent materials for NLO applications.

**Table 3. Calculated HOMO, LUMO, energy gap, ionization potential (IP) and electron affinity (EA) in (eV) of the isolated and halogen doped P3HT using B3LYP/6-311++G (d, p) basis Set**

| Molecules | HOMO (eV) | LUMO (eV) | IP (eV) | EA (eV) | $E_{gap}$ (eV) | Previous work [40] |
|---|---|---|---|---|---|---|
| Isolated P3HT | -5.0815 | -1.4379 | 5.0815 | 1.4379 | 3.644 | |
| Bromine doped P3HT | -5.0311 | -1.1845 | 5.0311 | 1.1845 | 3.85 | |
| Chlorine doped P3HT | -5.1329 | -1.5067 | 5.1329 | 1.5067 | 3.626 | |
| Fluorine doped P3HT | -5.0834 | -1.5379 | 5.0834 | 1.5379 | 3.545 | 4.35 |
| Iodine doped P3HT | -5.0806 | -1.5611 | 5.0806 | 1.5611 | 3.519 | |

**Table 4. Global chemical indices of the optimized structure of the isolated and substituted P3HT molecules using B3LYP/6-311++G (d) basis set**

| Molecules | η (eV) | ʃ(eV) | $\chi$ (eV) | μ (eV) | $\omega$(eV) |
|---|---|---|---|---|---|
| Isolated P3HT | 1.9137 | 0.5225 | -3.3012 | 3.3012 | 2.8473 |
| Bromine doped P3HT | 1.925 | 0.5195 | -3.1078 | 3.1078 | 2.5087 |
| Chlorine doped P3HT | 1.813 | 0.5516 | -3.3198 | 3.3197 | 3.0393 |
| Fluorine doped P3HT | 1.773 | 0.5642 | -3.3107 | 3.31067 | 3.0918 |
| Iodine doped P3HT | 1.7595 | 0.5683 | -3.1326 | 3.1326 | 2.7886 |

**Table 5. Thermodynamic properties of the optimized structure of isolated and substituted P3HT molecules using B3LYP/6-311++G (d) basis set**

| Molecules Positions | Isolated P3HT | | Bromine doped P3HT | | Chlorine doped P3HT | |
|---|---|---|---|---|---|---|
| | Cv (Kcal/Mol) | S (Kcal/Mol) | Cv (Kcal/Mol) | S (Kcal/Mol) | Cv (Kcal/Mol) | S (Kcal/Mol) |
| Electronic | 0.000 | 0.000 | 0.000 | 0.000 | 0.000 | 0.000 |
| Translational | 2.981 | 44.680 | 2.981 | 45.090 | 2.981 | 44.865 |
| Rotational | 2.981 | 38.995 | 2.981 | 39.559 | 2.981 | 39.317 |
| Vibrational | 145.245 | 180.491 | 147.821 | 182.057 | 147.550 | 183.952 |
| Total | 151.207 | 263.766 | 153.782 | 266.706 | 153.512 | 268.134 |
| Rotational Constants (GHz) | 0.09787 0.03268 | 0.04271 | 0.08048 0.02689 | 0.03579 | 0.08716 0.02946 | 0.03848 |
| ZPVE (Kcal/Mol) | 456.61913 | | 453.86700 | | 456.28354 | |

***Table 5. Continued…..***

| Molecules Positions | Isolated P3HT | | Fluorine doped P3HT | | Iodine doped P3HT | |
|---|---|---|---|---|---|---|
| | Cv (Kcal/Mol) | S (Kcal/Mol) | Cv (Kcal/Mol) | S (Kcal/Mol) | Cv (Kcal/Mol) | S (Kcal/Mol) |
| Electronic | 0.000 | 0.000 | 0.000 | 0.000 | 0.000 | 0.000 |
| Translational | 2.981 | 44.680 | 2.981 | 44.779 | 2.981 | 45.317 |
| Rotational | 2.981 | 38.995 | 2.981 | 39.148 | 2.981 | 39.853 |
| Vibrational | 145.245 | 180.491 | 146.296 | 182.285 | 147.761 | 183.674 |
| Total | 151.207 | 263.766 | 152.258 | 266.213 | 153.722 | 268.844 |
| Rotational Constants (GHz) | 0.09787 0.03268 | 0.04271 | 0.09513 0.03005 | 0.04095 | 0.07654 0.02388 | 0.03151 |
| ZPVE (Kcal/Mol) | 456.61913 | | 457.41568 | | 456.00368 | |

**Table 6. Non-linear optical properties (in electrostatic unit (esu)) and dipole moment in (DEBYE) of isolated and doped P3HT using B3LYP/6-311++G(d) basis Set**

| Molecule | $\mu_{tot}$ | $\langle\alpha\rangle$ | $\langle\Delta\alpha\rangle$ | $\beta_{tot}$ | $\gamma_{tot}$ |
|---|---|---|---|---|---|
| Isolated P3HT | 0.69378 | $-3.37\times10^{-23}$ | $3.77\times10^{-24}$ | $9.38\times10^{-31}$ | $-2.475\times10^{-17}$ |
| Bromine doped P3HT | 1.968475 | $-3.6534\times10^{-23}$ | $3.0767\times10^{-24}$ | $2.1222\times10^{-30}$ | $-8.3974\times10^{-20}$ |
| Chlorine doped P3HT | 2.405020 | $-3.6582\times10^{-23}$ | $3.1968\times10^{-24}$ | $2.9876\times10^{-30}$ | $-8.3834\times10^{-20}$ |
| Fluorine doped P3HT | 1.063097 | $-3.5023\times10^{-23}$ | $3.4274\times10^{-24}$ | $1.7456\times10^{-30}$ | $-7.9472\times10^{-20}$ |
| Iodine doped P3HT | 1.903425 | $-3.8396\times10^{-23}$ | $3.4758\times10^{-24}$ | $2.8803\times10^{-30}$ | $-8.9347\times10^{-20}$ |

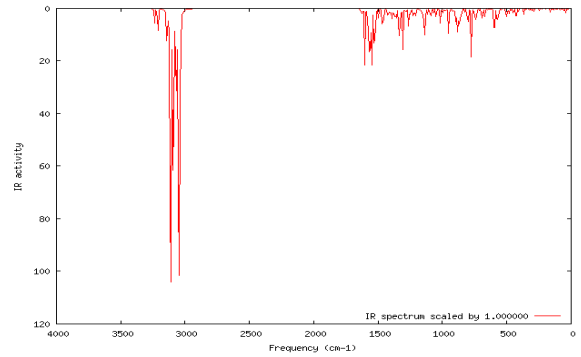


**(a) Chlorine doped P3HT**

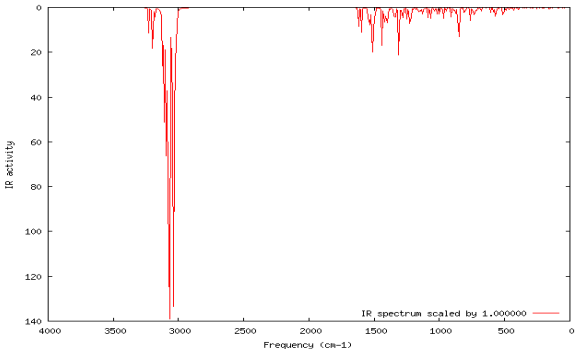


**(b) Bromine doped P3HT**

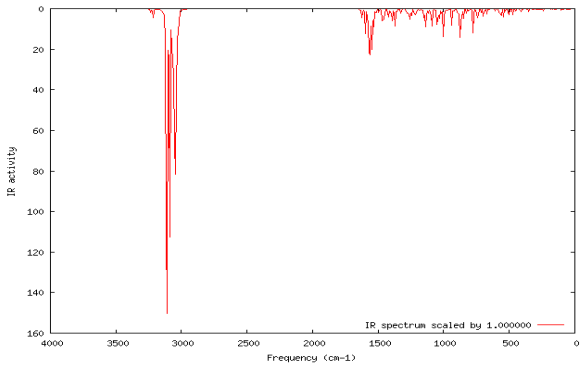


**(c) Fluorine doped P3HT**

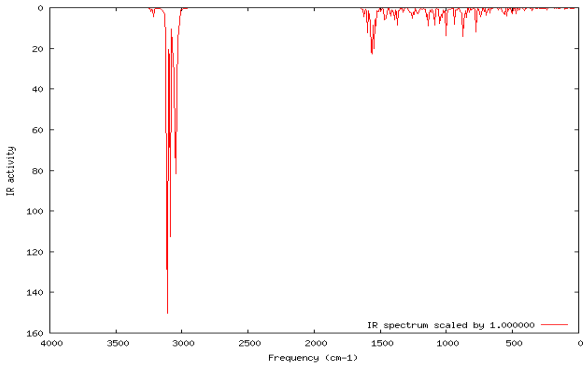


**(d) Iodine doped P3HT**

**Fig. 2 (a) -(d) IR spectra of isolated P3HT and substituted P3HT molecules**

## 4.6 Open-Circuit Voltage (VOC)

The open-circuit voltage of an organic solar cell is obtained from the difference between the HOMO of the donor and the LUMO of the electron acceptor, considering the energy loss during photo charge generation [44]. The theoretical values of $V_{OC}$ were calculated for the titled molecules using equation (15). For isolated P3HT, $V_{oc}$ values were calculated as $(1.3115eV)$ for PCBM $C_{60}$ and $(1.2415eV)$ for PCBM $C_{70}$. In bromine doped P3HT, the calculated values of $V_{oc}$ are $(1.2611\ \text{eV})$ for PCBM $C_{60}$ and $(1.1911\ \text{eV})$ for PCBM $C_{70}$. Similarly, $V_{oc}$ values for chlorine doped P3HT are $(1.3629\ \text{eV})$ for PCBM $C_{60}$ and $(1.2929\ \text{eV})$ for PCBM $C_{70}$. In fluorine doped P3HT, we have $V_{oc}$ values as $(1.3134\ \text{eV})$ for PCBM $C_{60}$ and $(1.2434\ \text{eV})$ for PCBM $C_{70}$. For the iodine doped P3HT, we obtained the calculated values of $V_{oc}$ as $(1.3106\ \text{eV})$ for PCBM $C_{60}$ and $(1.2415\ \text{eV})$ for PCBM $C_{70}$. These values are sufficient for possible efficient electron injection. Therefore, all the substituted molecules and isolated molecule can be used as sensitizers due to the fact that, the electron injection process from the excited molecule to the conduction band of PCEM derivatives and the subsequent regeneration is possible in an organic solar cell. We observed that the best values of Voc are $1.3629\ \text{eV}$ and $1.3134\ \text{eV}$ obtained in chlorine and fluorine doped P3HT respectively proves them to be more useful for organic solar cell application.

### 4.7 IR Intensities

The main idea of frequency analysis is to get vibrational modes connected with precise molecular structures of the measured compound [35]. Fig. 2 a-d show the graphical representation of the calculated vibrational frequencies and intensities of the isolated and substituted molecules. The graphs show that there is a slight increase in the peak values of frequencies for the titled molecule due to the presence of the halogens. From the graphs, the most intense frequencies for bromine doped P3HT and fluorine doped P3HT have values ranging between $3088.313\,cm^{-1}$ and $3118.618cm^{-1}$ with corresponding intensities of $76.4152km/mol$ and $89.3712km/mol$ respectively. At these frequencies, w =C-H stretch, s[broad] dimer OH, s Ar-H stretch and m =C-H stretch, s =C-H stretch were observed. While in chlorine and iodine doped P3HT we have the highest intense frequencies ranging between $3111.0826cm^{-1}$ and $3117.9295cm^{-1}$ .occurring at the intensity values of $63.1260km/mol$ and $64.1758km/mol$ respectively. At these frequencies, w =C-H stretch, s[broad] dimer OH, s Ar-H stretch and m =C-H stretch, s =C-H stretch were observed. Comparing the graphs presented, flouroP3HT has slightly higher peak values of frequencies (3118.6182 $cm^{-1}$) with corresponding intensities (89.3712 km/mol) than the rest of the molecules.

## 5. CONCLUSION

In this work, we reported the effects of doping halogens with Poly(3-hexylthiophene-2,5-diyl). The molecular geometry, the HOMO and LUMO, energy band gap, Global chemical reactivity parameters and non-linear optical properties of isolated P3HT and its mono-halogenated derivatives using B3LYP/6-311++G(d) basis set as implemented in Gaussian 09 software, were calculated and reported. The results show that the mono-halogenations of the studied molecule has positively improved the properties of the molecules compared to the isolated molecule. Since the lower the band gap, the much better is the performance of the molecule, the iodine doped P3HT has the lowest value of the energy gap of about $3.519\,eV$ compared to isolated P3HT which has a band gap of $3.644\,eV$ . Similarly, the results of first-order hyper-polarizability show that the chlorine and iodine doped P3HT are $2.9876 \times 10^{-30} esu$ and $2.8803 \times 10^{-30} esu$ respectively, which are found to be about eight times more than the value of urea, $0.3728 \times 10^{-30} esu$ which is commonly used for the comparison of NLO properties with other materials. These are remarkable improvements due to doping. We also discovered that the best values of $V_{oc}$ are $1.3629\,\mathrm{eV}$ and $1.3134\,\mathrm{eV}$ and are obtained in chlorine and fluorine doped P3HT respectively, thus proving them to be more useful for organic solar cell application. The absence of imaginary frequencies verified that the structures were at true minima and consequently in a more stable state. We also observed a slight increase in the peak values of the frequencies for the titled molecules due to the presence of the halogens. By and large, the work proved that doping P3HT with halogens has tuned the properties of this molecule for solar cell applications. Consequently, such halogens could also be applied to similar molecules for doping.

## COMPETING INTERESTS

Authors have declared that no competing interests exist.

## REFERENCES


1. Mohamed Si Bouzzine, Guillermo Salgado-Morán, Mohamed Hamidi, Mohammed Bouachrine, Alison Geraldo Pacheco, Daniel Glossman-Mitnik. DFT study of polythiophene energy band gap and substitution effects. Journal of Chemistry. 2015;1-12. Article ID 296386. Available:http://dx.doi.org/10.1155/2015/296386
2. Pesant S, Boulanger P, Cote M, Ernzerhof M. Ab initio study of ladder-type polymers: Polythiophene and polypyrrole. Chem. Phys. Lett. 2008;450:329–33.
3. Yen-Ju C, Sheng HY, Chain-Shu H. Synthesis of conjugated polymer for organic solar cell applications. Chem Rev; 2009.
4. Varun Vohraa, Osamu Notoyab, Tong Huanga, Masayuki Yamaguchia, Hideyuki Murataa. Nanostructured poly(3-hexylthiophene-2,5-diyl) films with tunable dimensions through self-assembly with polystyrene. JAIST. 2014;55(9):2213-2219. Available:http://dx.doi.org/10.1016/j.polymer.2014.03.030
5. Abu-Abdeen, Ayman M, Ayesh S, Abdullah A. Aljaafari. Physical characterizations of semi conducting conjugated polymer.CNT nanocomposites. J Polym Res. 2012;19: 9839. DOI: 10.1007/s10965-012-9839-z

6. Wenjing Hou, Yaoming Xiao, Gaoyi Han, Jeng-Yu Lin. The applications of polymers in solar cells: A Review. Polymers. 2019; 11:143.
DOI: 10.3390/polym11010143
7. Yang Bi, DQL, Boschloo G, Hagfeldt A, Johansson EMJ. Effect of different hole transport materials on recombination in $CH_3NH_3PbI_3$ perovskite-sensitized mesoscopic solar cells. J. Phys. Chem. Lett. 2013;4:1532–1536.
8. Edri E, Kirmayer S, Cahen D, Hodes G. High open-circuit voltage solar cells based on organic-inorganic lead bromide perovskite. J. Phys. Chem. Lett. 2013;4: 897–902.
9. Heo JH, Im SH. $CH_3NH_3PbI_3$/poly-3-hexylthiophen perovskite mesoscopic solar cells: Performance enhancement byLi-assisted hole conduction. Phys. Status Solidi RRL. 2014;8:816–821.
10. Habisreutinger SN, Leijtens T, Eperon GE, Stranks SD, Nicholas RJ, Snaith HJ. Carbon nanotube/polymer composites as a highly stable hole collection layer in perovskite solar cells. Nano Lett. 2014;14(10):5561-8.
DOI: 10.1021/nl501982b
11. Francisco C, Franco Jr. Tuning the optoelectronic properties of oligothiophenes for solar cell applications by varying the number of cyano and fluoro substituents for solar cell applications: A theoretical study. J. Chem. Res. 2020; 44(3-4):235–242.
Available:https://doi.org/10.1177/1747519819893884
12. Terence J Blaskovits, Thomas Bura, Serge Beaupre, Steven A. Lopez, Carl Roy, Julio de Goes Soares, Adam Oh, Jesse Quinn, Yuning Li, Alán Aspuru-Guzik, Mario Leclerc. A study of the degree of fluorination in regioregular poly(3-hexylthiophene), Macromolecules. 2016;50 (1):162–174.
DOI: 10.1021/acs.macromol.6b02365.
13. Kalpana G, Lim A. Ekanayake P, Iskandar PM. Cyanidin-based novel organic sensitizer for efficient dye-sensitized solar cells: DFT/TDDFT study. Int. J. Photoenergy; 2017. ID.8564293.
Available:https://doi.org/10.1155/2017/8564293.
14. Alamy ElA, Bourass M, Amina A, Mohammed H, Mohammed B. New organic dyes based on phenylenevinylene for solar cells: DFT and TD-DFT investigation. Karbala. Int. J. Mod. Sci. 2017;3:75-82.
15. Taoufik S, Bousselham K, Abbes L, Brahim. Photovoltaic energy conversion and optical properties of organic molecule based on aceanthraquinoxaline. Der pharma chemical. 2017;9(2): 37-42.
16. Yuanchao L, Lu M, Haibin W, Yuanzuo L, Jianping L. Design, electron transfer process, and opto-electronic property of solar cell using triphenylamine-based D- $\pi$-A architectures. Materials (Basels). 2019; 12(1):193.
DOI: 10.3390/ma12010193
17. Bourass M, Benjelloun AT, Hamidi M, Benzakour M, Mcharfi M, Sfaira M, Serein- Spirau F, Lere-Porte JP, Sotiropoulos JM, Bouzzine SM, Bouachrine. DFT theoretical investigation of -conjugated molecules based on thienopyrazine and different acceptor moieties for organic photovoltaic cells. J. Saudi Chem. Soc. 2016;20:S415-S425.
18. Hachi M, El Khattabi S, Fitri A, Benjelloun AT, Benzekour M, Mcharfi M, Hamidi M, Bouachrine M. DFT & TD-DFT studies of the -bridge influence on the photovoltaic properties of dyes based on thieno [2,3b] indole. J. Mater Environ. Sci. 2018;9:1200-1211.
19. Orio M, Pantazis DA, Neese F. Density Functional Theory. Photosynthesis Research. 2009;102:443-453.
Available:https://doi.org/10.1007/s11120-009-9404-8
20. Ravindram P. Introduction to density functional theory. Condens. Matter Phys; 2015.
21. Gidado AS, Salihu Abubakar, Shariff MA. "DFT, RHF and MP2 based study of the thermodynamic, electronic and non-optical properties of DNA nucleobases" Bayero Journal of Pure and Applied Sciences. 2017;10(1):115-127.
Available:http://dx.doi.org/10.4314/bajopas.v10i1.17
22. Bendjeddou A, Tahar A, Abdelkrim G, Didier V. Quantum chemical studies on molecular structure and stability descriptors of some p nitrophenyl tetrathiafulvalenes by density functional theory (DFT). Acta Chim.Pharm. Indica. 2016;6(2):32-44. ISSN 2277-288X.
23. Abdulaziz H, Gidado AS, Musa A, Lawal. Electronic structure and nonlinear optical properties of neutral and ionic pyrene and

its derivatives based on density functional theory. J Mater. Sci. Rev. 2019;2(3):1-13.
24. Tahar Abbaz, Amel Bendjeddou, Didier Villemin. Molecular structure, HOMO, LUMO, MEP, natural bond orbital analysis of benzo and anthraquinodimethane derivatives. Journal of Pharmaceutical and Biological Evaluations. 2018;5(2):27-39. Available:http://dx.doi.org/10.26510/23940859.pbe.2018.04
25. Haider Abbas, Mohd Shkir, AlFaify S. Density functional of spectroscopy, electronic structure, linear and non-linear optical properties of L-proline lithium chloride and L-proline lithium bromide monohydrate: For laser applications. Phys. Sci. int. J. 2015;(12):2342-2344.
26. Oyeneyin OE. Structural and solvent dependence of the electronic properties and corrosion inhibitive potentials of 1,3,4thiadiazole and its substituted derivatives: A theoretical investigation. Phys. Sci. int. J. 2017;16(2):1-8.
27. Khan MF, Bin Rashid R, Hossain A, Rashid MA. Computational study of solvation free energy, dipole moment, polarizability, hyperpolarizability and molecular properties of botulin, a constituent of Corypha taliera (Roxb.). Dhaka Univ. J. Pharm. Sci. 2017;16(1):1-8.
28. Suleiman AB, Abubakar Maigari, Gidado AS, Chifu E Ndikilar. "Density functional theory study of the structural, electronic, non-linear optical and thermodynamic properties of poly (3-Hexylthiophene-2, 5 -Diyl) in gas phase and in some solvents". PSIJ. 2022;26(4):34-51.
Article no.PSIJ.90692
DOI: 10.9734/PSIJ/2022/v26i430319
29. Chengteh Lee RGP, Weitao Yang. Development of the collesalvetti correlation-energy formula into a functional of the electron density. Phys. Rev. B. 1988;37(2):785–789.
30. Jamal M, Kamali SN, Yazdani A, Reshak AH. Mechanical and thermodynamical properties of hexagonal compounds at optimized lattice parameters from two-dimensional search of theequation of state. RSC Advances. 2014;4:57903-57915. Available:https://doi.org/10.1039/C4RA09358E
31. Frisch MJHM, Trucks GW, Schlegel HB, Scuseria GE, Robb MA, Cheeseman JR, Scalmani G, Barone V, Mennucci B, Petersson GA, Nakatsuji H, Caricato M, Li X, Hratchian PH, lzmaylov AF, Bloino J, Zheng G, Sonnenberg JL. Gaussian software. gaussian, INC. 2004;27.
32. Taura LS, Ndikilar CE, Muhammad A. Modeling the structures and electronic properties of Uraciland Thymine in gas phase and water. Modern Applied Science. 2017;11(11):01-11.
33. Wolf Van H. IR Pal 2.0: A tabledriven infrared application; 2010.
Available: http://home.kpn.nl/~vheeswijk
34. Mansur S, Yau D, Aliyu A, Tijjani RB, Abdullahi BA. Computational study of lawsonia inermis as potential and promising candidate for production of solar cell. European Journal of Advanced Chemistry Research; 2021.
ISSN 2684-4478.
35. Rabiu Nuhu Muhammad, Gidado AS. Investigating the effects of mono-halogen substitutions on the electronic, non-linear optical and thermodynamic properties of perylene based on density functional theory. Journal of Materials Science Research and Reviews. 2021;8(2):29-40. Article no.JMSRR.70860.
36. Kaloni T, Schreckenbach G, Freund M. Band gap modulation in polythiophene and polypyrrole-based systems. Sci; 2016.
Available:https://doi.org/10.1038/srep36554
37. Mason PE, Brady JW. Tetrahedrality and the relationship between collective structure and radial distribution functions in liquid water. J. Phys. Chem. 2007;111(20): 5669–5679.
38. Shukla A, Rajendra PT, Shukla KDP. Electronic state properties; Bond length and Bond angle of phenol and its some derivatives. Int. J. Chem. Sci: 2011;9(2): 627636.
39. Rajalakshmi K, Sharmila S. Spectroscopic studies and vibrational assignments, HOMO- LUMO, UV-VIS, NBO Analysis of Benzonitrile. International Journal of ChemTech Research. 2020;13(3):225239.
40. Terence J Blaskovits, Thomas Bura, Serge Beaupre, Steven A Lopez, Carl Roy, Julio de Goes Soares, Adam Oh, Jesse Quinn, Yuning Li, Alán Aspuru-Guzik, Mario Leclerc. A study of the degree of fluorination in regioregular poly(3-hexylthiophene). Macromolecules. 2016; 50(1):162-174.
DOI: 10.1021/acs.macromol.6b02365
41. Vidhya V, Austine A, Arivazhagan M. Quantum chemical determination of molecular geometries and spectral

investigation of 4-ethoxy-2, 3- difluoro benzamide, Heliyon. 2019;5(11): e02365.

42. Côme Damien Désiré Mveme, Fridolin Tchangnwa Nya, Geh Wilson Ejuh, Jean Marie, Bienvenu Ndjaka. "A Density Functional Theory (DFT) study of the doping effect on 4-[2-(2-N, N-dihydroxy amino thiophene) vinyl] benzenamine" SN Applied Sciences. 2021;3:317 Available:https://doi.org/10.1007/s42452-021-04277-1

43. Saji RS, Prasana JC, Muthu S, George J. Spectrochimica Acta Part A: Molecular Spectroscopy. 2020;226:117614.

44. Kumer A, Ahmed B, Sharif A, Al-mamun A. A theoretical study of aniline and nitrobenzene by computational overview. Asian J. Phys. Chem. Sci. 2017;4(2): 1–12.



*Peer-review history:*
*The peer review history for this paper can be accessed here:*
*https://www.sdiarticle5.com/review-history/92704*